Invest Clin 66(2): 205 - 216, 2025 https://doi.org/10.54817/IC.v66n2a07

Lycopene regulates the formation of calcium oxalate kidney stones by modulating reactive oxygen species(ROS) and NF-κB pathways.

Liangwen Ye, Yuhang Tang, Zhijie Zhang, Xiangyi Hou, Wei Xu, Xianghui Suo and Li Zhang

The First Clinical Medical College, Nanjing University of Chinese Medicine, Nanjing City, Jiangsu province, China.

Keywords: lycopene; renal tubular epithelial cells; oxalic acid; reactive oxygen species; apoptosis.

Abstract. This study aims to determine whether lycopene can reduce oxidative stress and inflammatory damage in HK-2 cell cultures induced by calcium oxalate crystallization through the modulation of reactive oxygen species (ROS) and the NF-κB signalling pathway. Cell cultures were divided into four groups: The control group, the Model group (COM + oxalic acid), and two Lycopene intervention groups (COM + oxalic acid + 5/10 μmol/L lycopene). After 24 hours of culture, viability, LDH, oxidative and anti-oxidative parameters, mitochondrial membrane potential, MCP-1, IL-6, apoptosis and related proteins, and activation and expression of NF-κB were determined by adequate methods. When compared to the control group, the model group exhibited decreased cell activity ($p<0.001$) and GSH and SOD antioxidant capacity ($p<0.05$), alongside a significant rise in LDH, MDA, and the release of inflammatory mediators MCP-1 and IL-6 ($p<0.05$). The levels of protein expression for NF-κB, OPN, Bax, Cyt C, and active Caspase-3 were increased ($p<0.05$), whereas Bcl-2 protein expression significantly diminished ($p<0.05$). The mitochondrial membrane potential decreased. Lycopene intervention reduced the damage to HK-2 cells ($p<0.05$), accompanied by decreased levels of LDH, MDA, and inflammatory factors MCP-1 and IL-6 ($p<0.05$), and increased GSH and SOD antioxidant capacity ($p<0.05$). The mitochondrial membrane potential was observed to increase. No significant changes were observed in the expression of NF-κB. The expressions of OPN, Bax, Cyt C, and Caspase-3 decreased ($p<0.05$), whereas the level of Bcl-2 protein expression increased. In conclusion, lycopene decreases cellular damage by inhibiting lipid peroxidation induced by calcium oxalate crystals and oxalate, enhancing intracellular antioxidant enzyme activity, modulating ROS and NF-κB inflammatory pathways, improving mitochondrial integrity, and exerting anti-inflammatory effects through the inhibition of the mitochondrial-mediated Bax/Caspase-3 signalling pathway.

Corresponding author: Li Zhang. The First Clinical Medical College. Nanjing University of Chinese Medicine. No. 138, Xianlin Road, Qixia District. Nanjing City 210023, Jiangsu Province, China. Tel: +86 13952009414. Email: LiiZZhang@outlook.com

El licopeno regula la formación de cálculos renales de oxalato cálcico modulando las vías de especies reactivas de oxígeno (ROS) y NF-κB.

Invest Clin 2025; 66 (2): 205 – 216

Palabras clave: licopeno; células epiteliales tubulares renales; ácido oxálico; especies reactivas de oxígeno; apoptosis.

Resumen. Este estudio tiene como objetivo determinar si el licopeno puede reducir el estrés oxidativo y el daño inflamatorio inducidos por la cristalización de oxalato de calcio en cultivos de células HK-2 a través de la modulación de especies reactivas de oxígeno (ROS) y las vías de señalización de NF-κB. Los cultivos celulares se dividieron en cuatro grupos: grupo control, grupo modelo (COM + ácido oxálico) y dos grupos de intervención con licopeno (COM + ácido oxálico + 5/10 μmol/L de licopeno). Después de 24 horas de cultivo, se determinaron la viabilidad, la LDH, los parámetros oxidativos y antioxidantes, el potencial de membrana mitocondrial, MCP-1, IL-6, la apoptosis y proteínas relacionadas, y la activación y expresión de NF-κB mediante métodos adecuados. En comparación con el grupo control, el grupo modelo mostró una actividad celular ($p<0,001$) y una capacidad antioxidante de GSH y SOD ($p<0,05$) disminuidas, junto con aumento significativo de LDH, MDA y la liberación de mediadores inflamatorios MCP-1 e IL-6 ($p<0,05$). Los niveles de expresión de proteínas para NF-κB, OPN, Bax, Cyt C y Caspasa-3 activa aumentaron ($p<0,05$), mientras que la expresión de la proteína Bcl-2 disminuyó significativamente ($p<0,05$). El potencial de membrana mitocondrial disminuyó. La intervención con licopeno redujo el daño celular ($p<0,05$), acompañada de una disminución de los niveles de LDH, MDA y los factores inflamatorios MCP-1 e IL-6 ($p<0,05$), y un aumento de la capacidad antioxidante de GSH y SOD ($p<0,05$). Se observó un aumento del potencial de membrana mitocondrial. No se observaron cambios significativos en la expresión de NF-κB. La expresión de OPN, Bax, Cyt C y Caspasa-3 disminuyó ($p<0,05$), mientras que la expresión de la proteína Bcl-2 aumentó. En conclusión, el licopeno disminuyó el daño celular al inhibir la peroxidación lipídica inducida por cristales de oxalato de calcio y oxalato, potenciar la actividad enzimática antioxidante intracelular, modular las vías inflamatorias de ROS y NF-κB, mejorar la integridad mitocondrial y ejercer efectos antiinflamatorios mediante la inhibición de la vía de señalización Bax/Caspasa-3 mediada por mitocondrias.

Received: 25-03-2025 *Accepted: 27-04-2025*

INTRODUCTION

Kidney stones constitute a common issue encountered in the urology field. Their widespread occurrence, high rates of recurrence, and the financial burden of treatment have significant implications for individuals and society [1]. One key factor contributing to kidney stone formation is the harm inflicted on renal tubular epithelial cells due to increased oxalate levels, with hyperoxaluria identified as a significant risk fac-

tor for developing urinary stones [2]. Exposure to elevated concentrations of oxalic acid over extended periods can trigger oxidative stress in these cells, leading to an overproduction of reactive oxygen species. This process may cause cellular harm, such as cell degeneration, apoptosis, and the exposure of the basement membrane of renal tubular epithelial cells [3], potentially worsening subsequent injuries. Following this, a series of cellular lipid peroxidation and inflammatory responses may occur [4]; as a result, antioxidants and anti-inflammatory medications are commonly employed to avert renal injury and the formation of kidney stones.

Lycopene (LYC), a vital carotenoid that falls under the classification of isoprenoid compounds, demonstrates properties such as anti-inflammatory, antioxidant, free radical scavenging, and immune modulation [5, 6]. Research indicates that lycopene may aid in relieving chronic prostatitis/chronic pelvic pain syndrome through its ability to diminish inflammation and oxidative stress by engaging the NF-κB, Nrf2, and MAPKs signalling pathways [7]. Nonetheless, no prior investigations have directly examined its protective effects against kidney damage caused by calcium oxalate stones. This study intends to explore the role and associated molecular mechanisms of LYC in the damage inflicted on renal tubular epithelial cells by oxalic acid and calcium oxalate crystals in vitro, thereby providing a theoretical foundation for utilizing anti-inflammatory and antioxidant agents, such as LYC, in the prevention and management of kidney stone disorders.

MATERIAL AND METHODS

Cells. HK-2 cells (purchased from BOSTER, catalogue number CX0044) were passed to the ninth passage.

Drugs and Reagents. *Lycopene* (Shanghai Yuanye Biotechnology Co., Ltd., product number B20378, purity ≥90%), *oxalic* (Shanghai Macklin Biochemical Technology Co., Ltd., product number O871905), *DMEMF-12* (1:1) basic medium (Gibco, USA, product number C11330500BT), *Cell Counting Kit-8* (Biosharp, product number BS350B), *Reduced glutathione* (GSH) assay kit, *Lactate dehydrogenase* (LDH) assay kit (Nanjing Jiancheng Bioengineering Institute Co., Ltd., product numbers A006-2-1 and A020-2-2), *Malondialdehyde* (MDA) Colorimetric Assay Kit, *Total Superoxide Dismutase* (T-SOD) Activity Assay Kit (Wuhan Elabscience Biotechnology Co., Ltd., product numbers E-BC-K028-M and E-BC-K020-M), In this study, we employed the *human IL-6 ELISA* kit and the *human MCP-1 ELISA* kit (Quanzhou Ruixin Biotechnology Co., Ltd., product numbers RX106126H and RX106032H), *Reactive oxygen species* (ROS) detection kit(Shanghai beyotimeBiotechnology Co., Ltd., product numbers S0033S). Additionally, *rabbit-derived antibodies* include *NF-κB p65*, *Osteopontin* (OPN), *Bax, Bcl-2, cytochrome C* (Cyt C), and *active-Caspase3*. *Secondary antibodies* include an *anti-mouse antibody* from Shanghai Beyotime Biotechnology Co., Ltd. (product numbers: AF5243, AF7662, A0216) and a *secondary rabbit antibody* from Proteintech Group, Inc. (batch numbers: 50599-2-Ig, 26593-1-AP, SA00001-2). Furthermore, a *mouse-derived GAPDH* antibody from BOSTER is identified by product numbers: PB9334, BM3937, and BM3876.

Instrumentation

In this research, the equipment used included the Series II Water Jacket CO2 cell culture incubator, the Infinite M1000 Pro full-wavelength microplate reader (Tecan, Switzerland), the Axio Vert A1 inverted fluorescence microscope (Zeiss, Germany), the Mini-Protean 3 Dodeca electrophoresis system, the ChemiDoc XPS+ all-in-one gel imaging system (Bio-Rad Company, USA), and the MoFlo XDP ultra-fast flow cytometer (BD Company, USA).

Method

LYC was dissolved in DMSO, and a blank culture medium was subsequently introduced

to formulate a storage solution with a concentration of 1000 μmol/L. The solution was passed through a microporous filter with a pore size of 0.22 μm and kept in a refrigerator at 4°C. Before beginning the experiment, the prepared LYC solution was administered to cultured cells in increasing concentrations (5, 10, 20, 40, 80, 100, 200, 500 μmol/L) to identify LYC's effective concentration and toxicity range. In a 96-well plate populated with HK-2 cells (1×104 cells/well), the effects of different LYC concentrations on HK-2 cytotoxicity were evaluated using the CCK-8 kit, with assessments made 24 hours after administration (refer to Table 1). Ultimately, lycopene concentrations of 5 μM and 10 μM were chosen for further experiments.

"A" Experimental grouping and intervention

The experimental groups were defined as follows: 1) Control group: cultured in basal medium for 24 hours; 2) Model group: cultured in basal medium containing oxalic (2 mmol/L) and COM (100 μg/mL) for 24 hours; 3) LYC I (5 μmol/L) group: treated with 5 μmol/L (LYC) in addition to the model group; 4) LYC II (10 μmol/L) group: treated with 10 μmol/L LYC in addition to the model group. These groups were utilized for subsequent experiments, including cell viability assessments, antioxidant capacity, inflammatory factors, reactive oxygen species, and Western blot analysis. Before the experiments, the original medium in the culture wells was removed, and serum-free medium was added to minimize the influence of proteins present in fetal bovine serum (FBS) on the experimental outcomes.

"B" CCK-8 assay to detect cell activity

HK-2 cells were plated in a 96-well plate at a density of 1 × 10 ^ 4 cells per well. After over 18 hours for complete attachment, the cells were allocated into groups for experimental interventions as specified in Section "A". Once the interventions were completed, the original culture medium was discarded and substituted with serum-free medium in every well. Subsequently, 100 μL of newly prepared culture medium and 10 μL of CCK-8 reagent were added, and the plate was incubated at 37°C for three hours. The absorbance (Ab) at 450 nm was recorded using a microplate reader. Each condition was evaluated in parallel within six replicate wells, and the experiment was conducted three times. The average value of Ab was computed, and cell activity was evaluated using the formula: Ab (experimental group) / Ab (control group) × 100%.

"C" Measurement of indicators related to antioxidant capacity

Cells were plated in a 6-well culture plate at a density of 2 x 10^5 cells per well until they adhered properly. The experimental groups aligned with those described previously (Experimental grouping). After a 24-hour incu-

Table 1. Effect of different concentrations of Lycopene on HK-2 cell activity.

Groups	Concentration /μmol/L	Relative cellular activity / %
Control group	0	100 ± 15.92
Lycopene group	5	98.26 ± 1.09
	10	94.75 ± 0.84
	20	88.13 ± 2.12
	40	86.92 ± 2.75
	80	85.02 ± 2.47
	100	79.82 ± 2.34
	200	69.27 ± 4.76
	500	31.39 ± 2.42

Data is expressed as $\bar{x}$ ± sd, n=3.

bation, cells from each group were collected, and the protein concentration was measured in centrifuge tubes. The instructions of the kit were followed to operate. Finally, the contents of lactate dehydrogenase(LDH), malondialdehyde (MDA), glutathione(GSH), and total superoxide dismutase(T-SOD) were measured in the cells using a Microplate reader at wavelengths of 450, 532, 405, and 450 nm and an ELISA kit was used for detection of IL-6, MCP-1 secretion.

"D" Cells were plated in a 6-well culture plate at a density of 2 x 10^5 cells per well until they adhered properly. The experimental groups aligned with those described in section "A". After a 24-hour incubation, the supernatant from each cell group was gathered into centrifuge tubes. Next, 50 μL from each group was transferred to the enzyme plate, following the instructions provided with the kit. Essential procedures included preparing three duplicate wells for every cell group, with the experiment conducted three times. The absorbance (Ab) measurement was taken at a wavelength of 450 nm to assess the levels of the inflammatory cytokines IL-6 and MCP-1.

"E" Observation of cellular ROS

Cells were plated in a 6-well culture dish at a density of 2 x 10^5 cells per well, adhering to the group allocations outlined before (A). After a 24-hour culture period, a ROS detection kit was utilized to evaluate the levels of intracellular ROS. Specifically, 10 μmol/L DCFH-DA, which was diluted in serum-free culture medium, was introduced in a dark environment. One mL of this fluorescent probe was administered, and the cells were incubated for 20 minutes. After incubation, the cells underwent three washes with 1 mL of serum-free culture medium, after which images were taken using an inverted fluorescence microscope.

"F" Western blot for protein expression in HK-2 cells

Cells were planted in a 6-well plate according to the method described in Section "D", then collected and denatured at high temperature. Electrophoresis was performed using the SDS gel system, followed by transfer to a PVDF membrane. The membrane was blocked with 5% skim milk at room temperature for 2 hours. The primary antibodies (NF-κB p65, OPN, Bax, Bcl-2, Cyt C, active-Caspase3, and GAPDH) were added and incubated at 4°C overnight. Subsequently, they were incubated with a secondary antibody at room temperature for 1.5 hours. The developing agent was added, and images were captured using an automatic gel imager. The ImageJ software was used to measure the gray value of each band and calculate the relative expression of target proteins in each group.

Statistical methods

All data were analyzed statistically with the use of GraphPad Prism 8.0.1 software. The outcomes are represented as $\bar{x} \pm SD$. A one-way ANOVA was utilized to compare several groups. A p-value lower than 0.05 was considered a statistically significant difference.

RESULTS

Comparison of cell activity and LDH in each group

Following 24 hours of treatment in the culture medium, the viability of cells in each group was assessed. The findings indicated a notable reduction in cell viability within the model group when juxtaposed with the control group ($p<0.001$), alongside a significant elevation in LDH levels ($p<0.001$). Conversely, cell viability in the LYC groups (5 μM, 10 μM) exhibited a marked increase compared to the model group ($p<0.05$), while LDH levels showed a significant decrease ($p<0.05$) (Table 2).

Comparison of antioxidant and anti-inflammatory capacities of HK-2 cells

The findings from the biochemical index assessments indicated a notable reduction in GSH levels within the model group when contrasted with the control group

Table 2. Comparison of cellular activity and intracellular lactate dehydrogenase content in each group.

Items	Control group	Model group	LYC (5μM)	LYC (10μM)
Cellular activity (%)	100	42±2.98[a]	60.37±3.44[b]	51.79±1.88[b]
LDH (U/g prot)	369.9±41.43	906±79.97[a]	483.7±70.8[b]	588.8±33.56[b]

Note: [a] is $p<0.001$ compared with the control group, and [b] is $p<0.05$ compared with the model group; as x, $\bar{x} \pm sd$, n=3. LDH: lactate dehydrogenase; LYC: Lycopene.

($p<0.05$). Conversely, MDA levels were found to have increased markedly ($p<0.05$). MDA levels saw a significant decline due to LYC treatment ($p<0.001$) (Table 3). Furthermore, when examining the model group, there was a notable surge in inflammatory cytokines IL-6 and MCP-1 compared to the control group ($p<0.05$). LYC administration at doses of 5 μM and 10 μM demonstrated an inhibitory effect on the secretion of IL-6 and MCP-1 relative to the model group ($p<0.05$) (Table 4).

Changes in intracellular ROS, mitochondrial membrane potential and apoptosis across different cell groups

In comparison to the control group, the model group exhibited enhanced green fluorescence and a reduced mitochondrial membrane potential. Following intervention with LYC (5 μM, 10 μM), the model group showed an increase in red fluorescence, a decrease in green fluorescence, and an improvement in mitochondrial membrane potential. Moreover, the generation of ROS was increased in the model group compared to the control group. However, after LYC intervention (5 μM, 10 μM), the model group demonstrated a decrease in ROS production (see Fig. 1 and Fig. 2). PI and Hoechst staining indicated that, in contrast to the control group, there was a rise in apoptotic cells within the model group, evidenced by intensified blue fluorescence. In comparison to the model group, treatment with LYC (5 μM, 10 μM) resulted in an improvement and a reduction in cell apoptosis, as shown by diminished blue fluorescence (Fig. 3).

Expression of inflammation and apoptosis-related proteins

The levels of NF-κB p65 and OPN in the model group were significantly elevated ($p<0.05$) compared to the control group, whereas LYC (5 μM, 10 μM) led to a decrease relative to the model group (Fig. 4). The expression levels of Bax, CytC, and active caspase3 were markedly increased ($p<0.05$) in the model group when compared to the control group, while Bcl-2 expression was significantly decreased ($p<0.05$). The LYC (5 μM, 10 μM) treatment group exhibited a downregulation in Bax, CytC, and active caspase3 expression, along with an upregulation in Bcl-2 expression compared to the model group (Table 5, Fig. 5).

DISCUSSION

The main goals in treating kidney stones include removing the stones, protecting kidney function, and tackling the root causes to reduce the likelihood of recurrence [8]. Thus, it is vital to identify specific pharmacological agents that target the condition's etiology for preventing and treating stones. The formation of kidney stones is a complicated process that entails the supersaturation of factors contributing to urolithiasis, harm to renal tubular epithelial cells, and the mechanisms of crystal adhesion, aggregation, nucleation, and growth [9]. A significant contributor to the development of kidney stones is oxalic acid. Elevated concentrations of oxalic acid may result in oxidative damage and initiate an inflammatory reaction in renal tubular epithelial cells [10].

Table 3. Comparison of indicators related to intracellular antioxidant capacity in each group.

Items	Control group	Model group	Lycopene (5μM)	Lycopene (10μM)
Glutathione (GSH, umol/g protein)	327.4±29.98	111.8±11.71[a]	212.1±21.1[b]	201.2±22.19[b]
Total superoxide dismutase (T-S0D, U/mg protein)	13.54±0.70	11.57±1.61	15.03±2.56	14.59±2.29
Malondialdehyde (MDA, nmol/mg protein)	2.166±0.3	22.89±0.441[a]	14.68±1.72[b]	15.43±0.85[b]

Note: [a] is $p<0.001$ compared with the control group, and [b] is $p<0.05$ compared with the model group. The above data was analyzed using one-way ANOVA. $\bar{x} \pm sd$, n=3.

Table 4. Effect of Lycopene on Interleukin-6 (IL-6) and Monocytechemotactic protein-1 (MCP-1) released from oxalic acid/calcium oxalate-induced HK-2 cells.

Groups	IL-6 (pg/mL)	MCP-1(pg/mL)
Control group	4.49 ± 0.44	9.78 ± 1.38
Model group	9.25 ± 0.46[a]	29.38 ± 3.51[a]
Lycopene (5μM)	5.42 ± 1.49[b]	7.71 ± 6.10[b]
Lycopene (10μM)	5.28 ± 1.51[b]	11.84 ± 4.85[b]

Note: [a] is $p<0.001$ compared with the control group, and [b] is $p<0.05$ compared with the model group. The above data was analyzed using one-way ANOVA; ($\bar{x} \pm sd$, n=3).

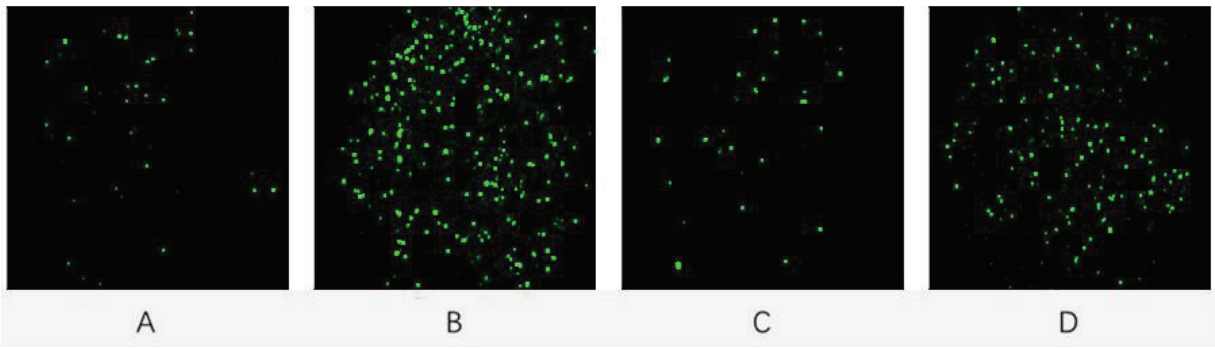

Fig. 1. Effect of LYC on oxalic acid/calcium oxalate crystal-induced intracellular reactive oxygen species ROS in HK-2 cells. A. control group; B. model group; C. LYC (5 μM); D. LYC (10 μM) group (Immunofluorescence, x100).

An expanding array of studies has demonstrated a relationship between inflammation, oxidative stress, and kidney stone formation [4, 11]. Hence, investigating effective anti-inflammatory and antioxidant mechanisms is crucial for alleviating kidney injury associated with calcium oxalate stones.

Malondialdehyde (MDA) is the end product generated from the peroxidation of cellular lipids. The levels of MDA offer valuable information regarding the degree of lipid peroxidation in the body, thereby acting as an indirect indicator of cellular damage.

Although free radicals can inflict considerable harm, human cells also harbor substances that neutralize these free radicals. Among these protective agents, super-

oxide dismutase (SOD) stands out as a key antioxidant enzyme that aids in reducing the damage inflicted by oxygen-derived free radicals [12]. A reduction in SOD activity indicates a lower ability of the organism to combat free radical-induced damage, implying that the organism may be undergoing oxidative stress. For example, continuous exposure to elevated levels of oxalic acid can promote the production of free radicals, which initiate lipid peroxidation within biological membranes.

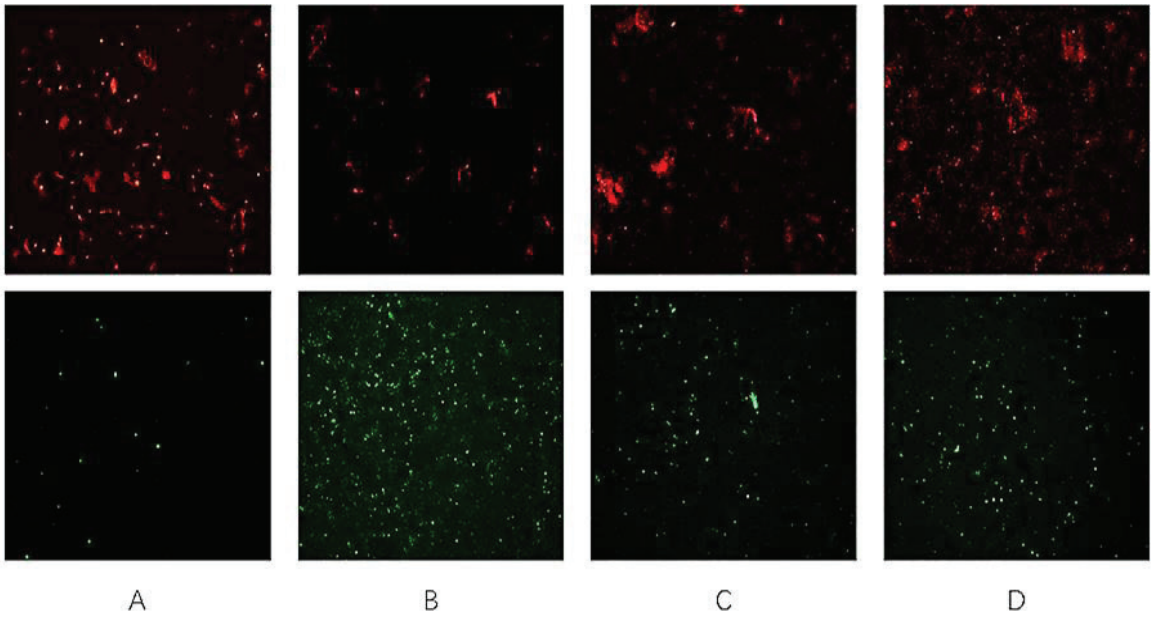

Fig. 2. Effect of LYC on mitochondrial membrane potential induced by oxalic acid/calcium oxalate crystals in HK-2 cells. A. control group; B. model group; C. LYC (5 μM); D. LYC (10 μM) group (Immunofluorescence, x100).

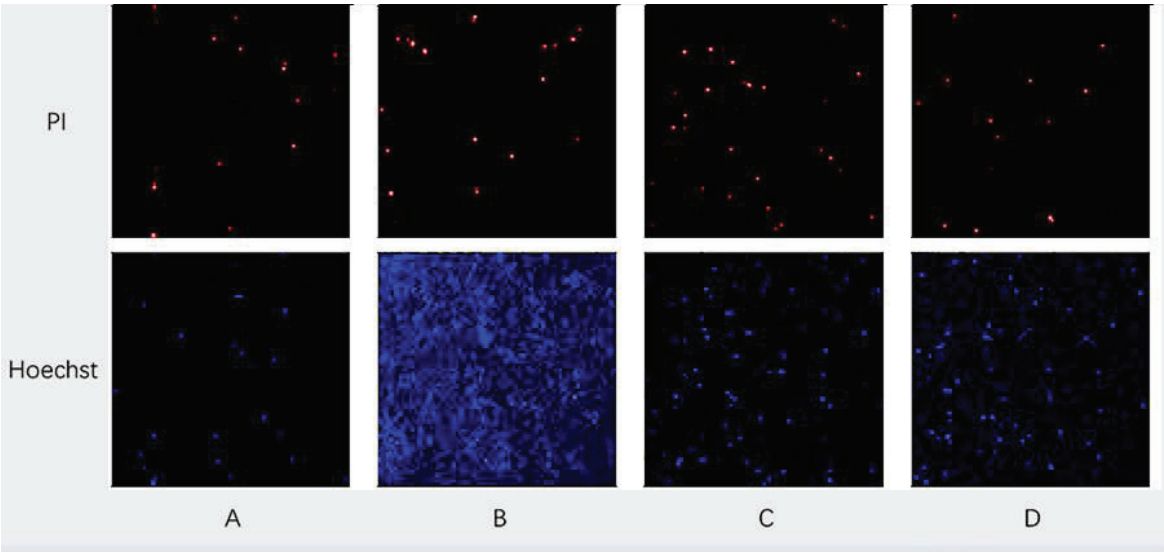

Fig. 3. Effect of LYC on the apoptotic profile of HK-2 cells induced by oxalic acid/calcium oxalate crystals. A. control group; B. model group; C. LYC (5 μM); D. LYC (10 μM) group. PI: propidium iodide (Immunofluorescence, x100).

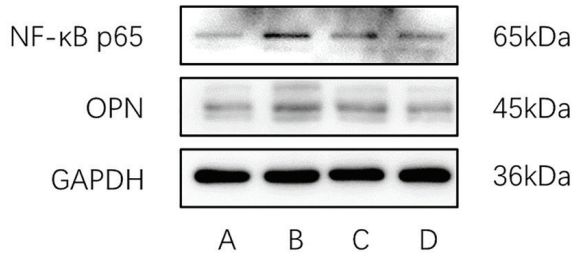

Fig. 4. LYC ameliorates oxalic acid/calcium oxalate crystal-induced changes in inflammation-associated protein levels in HK-2 cell injury.

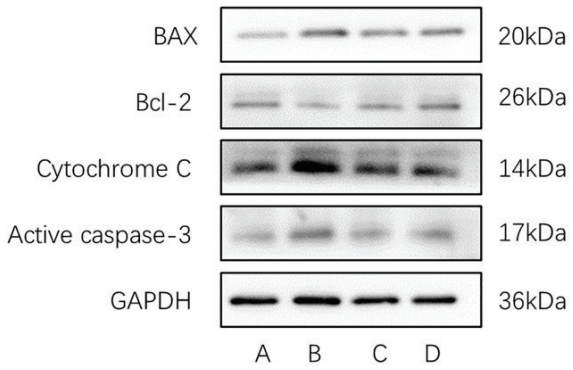

Fig. 5. Changes in the levels of mitochondrial damage-related proteins in HK-2 cells.

Table 5. Relative expression of proteins related to inflammation and mitochondrial damage in cells of each group.

Items	Control group	Model group	Lycopene (5μM)	Lycopene(10μM)
P65	0.708±0.077	1.014±0.053[a]	0.807±0.163	0.782±0.229
Osteopontin (OPN)	0.546±0.70	0.864±0.006[a]	0.746±0.260	0.642±0.127[b]
BAX	0.427±0.062	1.109±0.205[a]	0.734±0.221	0.542±0.203[b]
Bcl-2	1.13±0.301	0.466±0.228[a]	0.536±0.261	0.544±0.245
Cytochrome C (Cyt C)	0.539±0.066	2.242±0.428[a]	0.930±0.264[b]	0.775±0.490[b]
Active caspase3	0.355±0.155	1.16±0.231[a]	0.585±0.212[b]	0.771±0.165

Note: [a] is $p<0.001$ compared with the control group, and [b] is $p<0.05$ compared with the model group. The above data was analyzed using one-way ANOVA.

This chain of events may result in changes to the ultrastructural integrity of cell membranes, enable cellular penetration, inflict harm on mitochondria and DNA, and ultimately lead to cell necrosis and apoptosis[13]. These experimental findings reveal that the oxidative damage to HK-2 cells induced by oxalic acid/calcium oxalate is significant, as evidenced by compromised cell proliferation, decreased cell viability, heightened release of lipid peroxidation byproducts like MDA and LDH, along with lower levels of antioxidant enzymes such as SOD and GSH. Following treatment with LYC, we noted an enhancement in cell viability, reduced oxidative injury, and increased antioxidant activity.

Reactive oxygen species (ROS) are recognized as primary regulators of oxidative stress and identified as significant contributors to the damaging effects of pathological stone formation [14]. The role of the NF-κB signaling pathway is critical in facilitating intrarenal inflammation mediated by oxidative stress [15]. The significant production of ROS caused by oxidative stress can additionally activate various signalling pathways associated with inflammation, creating diverse inflammatory mediators and promoting the buildup of inflammatory cells, thus triggering and enhancing the inflammatory response. Studies show that heightened oxalic acid levels can provoke the activation of the NF-κB intracellular signalling pathway, which leads to an increased expression of inflammatory factors like OPN and MCP-1/IL-6, ultimately resulting in the infiltration of inflammatory cells and causing interstitial damage [4]. Monocyte chemotactic protein-1 is an essential inflammatory mediator contributing to the inflammatory

reactions linked to calcium oxalate kidney stones. Under standard physiological conditions, renal tissue cells only produce a minimal amount of MCP-1. However, when oxalic acid or calcium oxalate crystals precipitate in urine due to supersaturation, these substances can damage and stimulate these cells, leading to a substantial increase in MCP-1 production, subsequently attracting monocytes into the inflamed tissue [16]. Boonla et al. [17] compared MCP-1 and IL-6 mRNA expression levels in kidney tissues adjacent to stones and those in normal kidneys. Their findings indicated more severe tubular damage in the tissues surrounding the stones and significantly reduced expression levels of MCP-1 and IL-6 compared to normal kidney tissues. This observation implies that MCP-1 and IL-6 may be involved in advancing kidney stone disease.

Furthermore, during cellular damage, various negatively charged molecules—including osteopontin (OPN), hyaluronic acid (HA), and CD44 [18]—are showcased on the cell surface. These molecules can bind to Ca2+ ions and attach to positively charged calcium oxalate crystals. The adhering crystals can trigger cellular production of free radicals, further harming the renal epithelium via lipid peroxidation, thus heightening the possibility of kidney stone formation. The study utilized ELISA experiments to show that MCP-1 and IL-6 release were elevated in the model group, while LYC was found to have a protective effect. Western blot analyses indicated that NF-κB and OPN levels were upregulated in the model group relative to the control group; however, their expression was reduced after LYC treatment. In addition, a combined analysis of reactive oxygen species levels in cells revealed that LYC could ameliorate the intrarenal ROS levels triggered by oxalic acid/calcium oxalate crystals in HK-2 cells, effectively inhibiting the NF-κB signalling pathway and thereby diminishing the intrarenal inflammatory response.

The deposition of calcium oxalate crystals may also cause damage to mitochondria by increasing cellular ceramide levels. Mitochondrial abnormalities or oxidative stress can trigger the initiation of cell apoptosis programs. The family of Bcl-2 proteins is crucial in governing mitochondrial permeability to various proteins and the permeabilization of the outer mitochondrial membrane, playing an essential role in the intrinsic apoptosis pathway. Bax and Bcl-2 are pro-apoptotic and anti-apoptotic agents, respectively [19]. While Bcl-2 shields cells from mitochondrial injury and suppresses apoptosis, Bax enhances the permeability of the mitochondrial membrane, facilitating the release of cytochrome C (Cyt C) [20]. This sequence of events leads to an increase in hydrogen peroxide production, a decrease in glutathione peptide levels, and a drop in mitochondrial membrane potential, coupled with the liberation of apoptotic factors into the cytosol, which ultimately activates caspase-3 and induces cell death [21]. The expression levels of proteins associated with the mitochondrial pathway were evaluated in this study.

Results indicate that treatment with oxalic acid/calcium oxalate crystals led to an upregulation of Bax, Cyt C, and active-caspase3, while a downregulation of Bcl-2 was observed. Following the intervention with LYC, improvements in cell apoptosis were noted. These findings imply that LYC may mitigate HK-2 cell apoptosis by inhibiting the Bax/caspase3 signalling pathway.In conclusion, LYC demonstrates a significant ability to reduce oxidative stress and inflammatory responses in HK-2 cells, enhances cellular health, and may operate through the modulation of the ROS/NF-κB inflammasome pathway while also mitigating mitochondrial damage by inhibiting the Bax/caspase3 signalling pathway associated with mitochondria. This research offers an initial insight into the potential mechanisms by which LYC could aid in the clinical prevention and treatment of kidney stones, thereby opening new avenues

and concepts for addressing calcium oxalate kidney stones and the clinical utilization of LYC and analogous medications. Nonetheless, as the investigation primarily focuses on cellular models, it may not wholly replicate the mechanisms involved in the human body, indicating that the study has inherent limitations, warranting further exploration and validation.

ACKNOWLEDGEMENTS

Thanks for the support from the Special Project for the Promotion of Department Heads of Traditional Chinese Medicine Hospitals in Jiangsu Province.

Funding

This study was supported by the Special Project for the Promotion of Department Heads of Traditional Chinese Medicine Hospitals in Jiangsu Province(Y2021Z19).

Ethics approval and consent to participate

Not applicable, our study utilizes commercially available cell lines, and the Nanjing University of Chinese Medicine does not mandate ethics review for research conducted with such cell lines. So, there are no ethical issues or conflicts of interest.

Availability of data and materials

The datasets used and/or analyzed during the current study are available from the corresponding author on reasonable request.

Conflict of interests

All authors declare no conflict of interest.

Number ORCID of authors

- Liangwen Ye (LY): 0009-0003-9780-4688
- Yuhang Tang (YT): 0009-0009-6263-0570
- Zhijie Zhang (ZZ): 0009-0006-8535-0748
- Xiangyi Hou (XH): 0009-0004-5185-6965
- Wei Xu. (WX): 0009-0004-0948-5822
- Xianghui Suo (XS): 0009-0008-1688-0694
- Li Zhang (LZ): 0009-0002-2514-6690

Authors' Contributions

LY and YT designed the study; data acquisition, analysis, and interpretation were conducted by ZZ and XH; the manuscript underwent revision by LY, WX, and XS; LZ also played a role in the article's revision. Each author contributed to the paper and approved the final version submitted.

REFERENCES

1. **Tan S, Yuan D, Su H, Chen W, Zhu S, Yan B**, et al. Prevalence of urolithiasis in China: a systematic review and meta-analysis. BJU Int. 2024;133:34-43. *10.1111/bju.16179.*
2. **Qin B, Wang Q, Lu Y, Li C, Hu H, Zhang J**, et al. Losartan ameliorates calcium oxalate-induced elevation of stone-related proteins in renal tubular cells by inhibiting NADPH oxidase and oxidative stress. Oxid Med Cell Longev. 2018;2018:1271864. *10.1155/2018/1271864.*
3. **Kang J, Sun Y, Deng Y, Liu Q, Li D, Liu Y**, et al. Autophagy-endoplasmic reticulum stress inhibition mechanism of superoxide dismutase in the formation of calcium oxalate kidney stones. Biomed Pharmacother. 2020;121:109649. *10.1016/j.biopha.2019.109649.*
4. **Khan SR.** Reactive oxygen species as the molecular modulators of calcium oxalate kidney stone formation: evidence from clinical and experimental investigations. J Urol. 2013;189:803-11. *10.1016/j.juro.2012.05.078.*

5. **Liu CB, Wang R, Yi YF, Gao Z, Chen YZ**. Lycopene mitigates β-amyloid induced inflammatory response and inhibits NF-κB signaling at the choroid plexus in early stages of Alzheimer's disease rats. J Nutr Biochem. 2018;53:66-71. *10.1016/j.jnutbio.2017.10.014.*
6. **Caseiro M AA, Costa A, Creagh-Flynn J, Johnson M, Simões S**. Lycopene in human health. LWT. 2020;127. *10.1016/j.lwt.2020.109323.*
7. **Zhao Q, Yang F, Meng L, Chen D, Wang M, Lu X,** et al. Lycopene attenuates chronic prostatitis/chronic pelvic pain syndrome by inhibiting oxidative stress and inflammation via the interaction of NF-κB, MAPKs, and Nrf2 signaling pathways in rats. Andrology. 2020;8:747-755. *10.1111/andr.12747.*
8. **Sixing Y ZY**. Reconsiderations of several key issues in the treatment of urolithiasis. Chinese J of Urol. 2018;9. *10.3760/cma.j.issn.1000-6702.2018.09.002.*
9. **Thongboonkerd V**. Proteomics of crystal-cell interactions: a model for kidney stone research. Cells. 2019;8. *10.3390/cells8091076.*
10. **Liu Q, Liu Y, Guan X, Wu J, He Z, Kang J**, et al. Effect of M2 macrophages on injury and apoptosis of renal tubular epithelial cells induced by calcium oxalate crystals. Kidney Blood Press Res. 2019;44:777-791. *10.1159/000501558.*
11. **Mulay SR, Kulkarni OP, Rupanagudi KV, Migliorini A, Darisipudi MN, Vilaysane A,** et al. Calcium oxalate crystals induce renal inflammation by NLRP3-mediated IL-1β secretion. J Clin Invest. 2013;123:236-246. *10.1172/jci63679.*
12. **Zabłocka A, Janusz M**. [The two faces of reactive oxygen species]. Postepy Hig Med Dosw (Online). 2008;62:118-124.
13. **Joshi S, Khan SR**. Opportunities for future therapeutic interventions for hyperoxaluria: targeting oxidative stress. Expert Opin Ther Targets. 2019;23:379-391. *10.1080/14728222.2019.1599359.*
14. **Umekawa T, Tsuji H, Uemura H, Khan SR**. Superoxide from NADPH oxidase as second messenger for the expression of osteopontin and monocyte chemoattractant protein-1 in renal epithelial cells exposed to calcium oxalate crystals. BJU Int. 2009;104:115-120. *10.1111/j.1464-410X.2009.08374.x.*
15. **Patel M, Yarlagadda V, Adedoyin O, Saini V, Assimos DG, Holmes RP**, et al. Oxalate induces mitochondrial dysfunction and disrupts redox homeostasis in a human monocyte derived cell line. Redox Biol. 2018;15:207-215. *10.1016/j.redox.2017.12.003.*
16. **Zuo L, Tozawa K, Okada A, Yasui T, Taguchi K, Ito Y**, et al. A paracrine mechanism involving renal tubular cells, adipocytes and macrophages promotes kidney stone formation in a simulated metabolic syndrome environment. J Urol. 2014;191:1906-1912. *10.1016/j.juro.2014.01.013.*
17. **Boonla C, Hunapathed C, Bovornpadungkitti S, Poonpirome K, Tungsanga K, Sampatanukul P,** et al. Messenger RNA expression of monocyte chemoattractant protein-1 and interleukin-6 in stone-containing kidneys. BJU Int. 2008;101:1170-1177. *10.1111/j.1464-410 X.2008.07461.x.*
18. **Khan SR, Joshi S, Wang W, Peck AB**. Regulation of macromolecular modulators of urinary stone formation by reactive oxygen species: transcriptional study in an animal model of hyperoxaluria. Am J Physiol Renal Physiol. 2014;306:F1285-1295. *10.1152/ajprenal.00057.2014.*
19. **Lalier L, Vallette F, Manon S**. Bcl-2 family members and the mitochondrial import machineries: The roads to death. Biomolecules. 2022;12. *10.3390/biom12020162.*
20. **Hu L, Chen M, Chen X, Zhao C, Fang Z, Wang H**, et al. Chemotherapy-induced pyroptosis is mediated by BAK/BAX-caspase-3-GSDME pathway and inhibited by 2-bromopalmitate. Cell Death Dis. 2020;11:281. *10.1038/s41419-020-2476-2.*
21. **Khan SR**. Reactive oxygen species, inflammation and calcium oxalate nephrolithiasis. Transl Androl Urol. 2014;3:256-276. *10.3978/j.issn.2223-4683.2014.06.04.*